

Tuning Energetic Levels in Nanocrystal Quantum Dots through Surface Manipulations

Michal Soreni-Harari,[†] Nir Yaacobi-Gross,[†] Dov Steiner,[‡] Assaf Aharoni,[§]
Uri Banin,[§] Oded Millo,[‡] and Nir Tessler*,[†]

The Zisapel Nano-electronics center, Department of Electrical Engineering, Technion - Israel Institute of Technology, Technion City, Haifa 32000, Israel, and Racah Institute of Physics, the Center for Nanoscience and Nanotechnology, Department of Physical Chemistry, The Hebrew University, Jerusalem, 91904, Israel

Received December 10, 2007

ABSTRACT

We demonstrate tuning of the electronic level positions with respect to the vacuum level in colloidal InAs nanocrystals using surface ligand exchange. Electrochemical as well as scanning tunneling spectroscopy measurements reveal that the tuning is largely dependent on the nanocrystal size and the surface linking group, while the polarity of the ligand molecules has a lesser effect. The implications of affecting the electronic system of nanocrystal through its capping are illustrated through prototype devices.

Nanoscale inorganic materials display unique size, shape, and composition dependent electronic and optical properties. These tunable properties have been implemented in hybrid organic–inorganic devices where nanocrystals were interfaced with semiconducting polymers. Two main device types were demonstrated. First, light emitting diodes (LEDs) utilizing size-dependent emission of the nanocrystals to yield tunable electroluminescence^{1–5} and second, photovoltaic devices (PVs) and photodetectors that utilize strong absorption cross sections and large interface areas between the polymer and nanocrystals required for charge separation.^{6–10} Nanocrystals (NCs) are capped with a surfactant layer that is necessary for their solution-based synthesis and is also pertinent to their chemical processability, which is a key advantage in device production. Yet, utilization of inorganic NCs in device applications requires an appropriate manipulation of the surrounding capping layer of the NCs due to fabrication and performance requirements. Perhaps the most important factor in hybrid polymer–NC devices is the relative position of the energy levels of the host polymer and the guest NC.^{11,12} In LEDs, the conduction and valence bands of the NC should be enclosed within the polymer bands (known as type I band alignment, see Figure 1a). Conversely, a staggered band alignment is required in a solar cell (type II band alignment, Figure 1b). Band alignments

are not easily tunable as they are determined mostly by the material parameters, and in particular for the inorganic NCs there is little flexibility in determining their positions.

In this paper, we show that the NC energy levels positions are largely dependent on the ligand. Understanding this dependency leads to the ability to tune the energy levels (Figure 1a,b) using ligand exchange (Figure 1c). To this end, we report on detailed studies of the highest occupied molecular orbital (HOMO) level shifting of InAs semiconductor (SC) NCs using both voltammetry on NC ensembles and scanning tunneling spectroscopy (STS) measurements on single NCs. We supplement this study with a demonstration of the use of the energy level shifting effect, which showed a dramatic improvement in device performance of bilayer InAs NCs/poly(p-phenylene vinylene) (PPV) PV devices.

In infinite size two-dimensional (2D) inorganic surfaces, grafting of organic molecules has been extensively studied in the context of band alignment. The adsorption of organic molecules can lead to the formation of microscopic surface dipole that modifies the energy level alignment at the interface. This effect was demonstrated to tune the surface and interface properties in bulk inorganic semiconductor devices^{13–15} as well as in organic optoelectronic devices.^{16–18} In general, the dipole moments of the free molecular skeleton derivatives were found to correlate with the changes in the magnitude and direction of the semiconductor work function and the effective barrier heights. There are also some indications that the shift in the energy level alignment is

* Corresponding author. E-mail: nir@ee.technion.ac.il.

[†] Technion - Israel Institute of Technology.

[‡] Racah Institute of Physics and the Center for Nanoscience and Nanotechnology, The Hebrew University.

[§] Department of Physical Chemistry and the Center for Nanoscience and Nanotechnology, The Hebrew University.

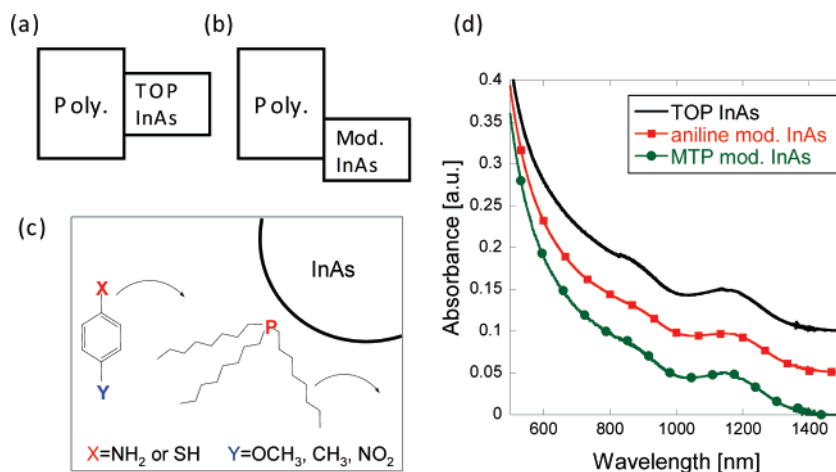


Figure 1. Energy levels tuning through surface exchange. Schematic energy level diagram of the type I (a) and type II (b) alignment. (c) Modification of NC surface properties. Ligand exchange of TOP-capped InAs NC with a *p*-phenylene ligand bearing a binding functionality (X) and a variable polar terminal group (Y). (d) Absorbance measurements of TOP-capped InAs NCs sample in toluene (solid) in comparison to its surface-modified aniline (squares) and MTP (circles) samples in (tetrahydrofuran) THF. The actual spectra are identical but are shifted for clarity.

dependent on the binding group of the ligand and the interacting substrate atoms.

In light of these significant effects induced by organic ligands on 2D surfaces, one could expect that in NCs, which are characterized by exceptionally large surface to volume ratios (for example, a 2 nm InAs dot has about half of its atoms on the surface), capping ligand design could allow for band tuning. Surface ligands were previously shown to affect several important properties of the particles such as their processibility, photostability, assembly, spectroscopic properties, as well as redox activity.^{19–27} It was also reported that upon ligand removal a signature of surface states appeared in the tunneling spectra of isolated NCs.²⁸ However, band position tuning using surface ligands was not reported for semiconductor NCs systems. Indeed, applying the principles learned in this context from infinite surfaces to the surface of nanosize particles is not necessarily straight forward because the small size and high symmetry of the NCs can give rise to competing interactions as well as screening effects.²⁹

Although the grafting of organic molecules onto 2D surfaces has been extensively studied, in the first step of our study better understanding of the contribution of the organic molecular layer in SC NCs is sought. To this end, we employed chemical modification of trioctylphosphine (TOP)-capped InAs quantum dots (QDs) using various para-phenylene skeleton molecules in which one end is a binding functionality (–X), and the other end is a terminal group with electron withdrawing/donating power (–Y) (see Figure 1c). We studied a series of molecules bearing the same binding group (thiol-containing ligands) with different auxiliary polar substituents. In addition to that, ligands bearing different binding groups (amine and thiol-containing ligands) were examined.

The surface modification via ligand exchange technique of the original TOP-capped InAs QDs with the new ligands was verified using Fourier transform infrared spectroscopy (FTIR). The measurements indicated that the modifying

ligands bearing a thiol group, 4-nitrothiophenol (NTP), 4-methoxythiophenol (MoTP), and 4-methylthiophenol (MTP), were attached to the NCs via the thiolate group. In addition, a comparison of the free amine containing ligand, the aniline, to its exchange-reaction product indicated the ligand's attachment to the NCs. While there is a clear evidence for the exchange reaction, there is also some indication that the exchange did not replace 100% of the TOP molecules on the NC surface.

To verify that the QDs did not degrade as a result of the exchange procedure, absorbance measurements were performed. For example, the comparison between the TOP-capped QD with the aniline-modified and the MTP-modified QDs shows (Figure 1d) that the modified NCs have exactly the same absorption spectrum indicating that the modified NCs retained their quantum-confined characteristics.

Two complementary techniques were used to study the energy level tuning following ligand exchange. The first technique employed voltammetry measurements using NCs dispersed in nonaqueous solutions to determine their HOMO levels. Because optical measurements revealed that the band gaps were not changed as a result of the surface modifications, we focused the study on HOMO level positioning. This choice was encouraged by the observation that electrogenerated oxidized species of NCs are more stable than the reduced ones.³⁰

The cyclic voltammogram of TOP-capped InAs NCs is shown in Figure 2a. The anodic wave along the positive potential scale versus Ag/AgNO₃ is ascribed to the HOMO level.¹² In addition to cyclic voltammetry (CV), we employed differential pulse voltammetry (DPV), which enables higher sensitivity. A reproducible response was obtained upon measuring different samples. Figure 2b shows the DPV signal (full line) as well as the net NCs signal (dashed line) obtained after subtracting the background. We note that the TOP–InAs have a rather broad signal. Because of the semi-insulating nature of the TOP, we had to use up to 1 order of magnitude higher concentration compared to the substituted

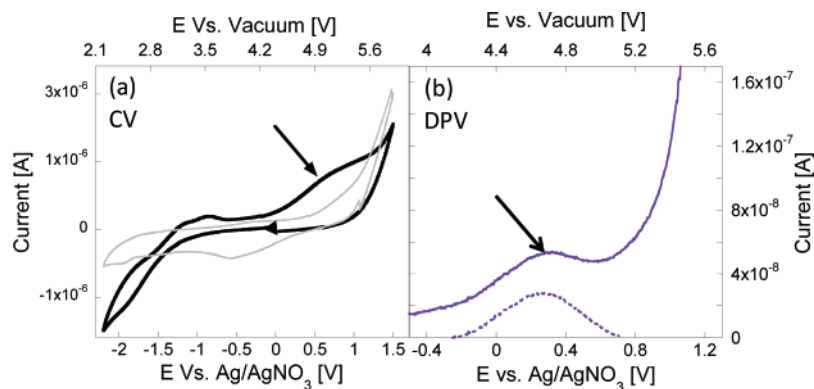


Figure 2. TOP-capped InAs NCs voltammograms (a) CV curves of 4.4 nm diameter (1130 nm) NCs (black) and the electrolyte solution (gray) at 0.1 V/s. (b) DPV curves of the TOP-InAs (solid) and the signal after subtracting the background (dashed); potential was swept from negative to positive. NCs samples were dispersed in THF + 0.1 M TBAPF₆. The peaks ascribed to the HOMO levels of the NCs are designated with arrows.

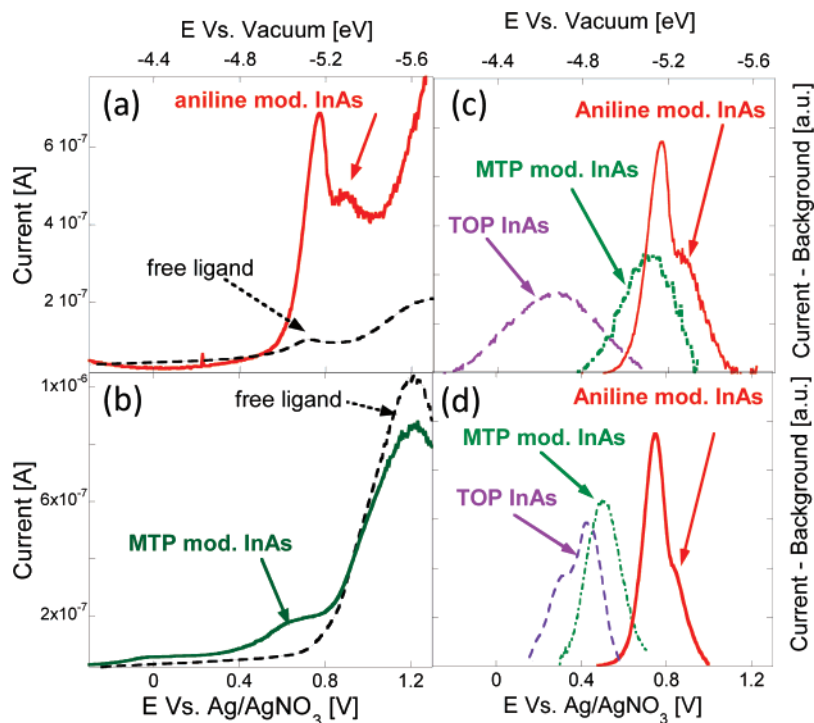


Figure 3. HOMO levels deduced from DPV. (a,b) Show the DPV of modified InAs NCs samples (4.4 nm diameter) in comparison to their corresponding unbound ligand dissolved in THF + 0.1 M TBAPF₆. (a) Aniline-modified InAs NCs (solid), unbound aniline ligand (dashed). (b) MTP-modified InAs NCs (solid), unbound MTP ligand (dashed). Potential was swept from negative to positive. (c,d) Show the background subtracted signal of TOP, MTP, and aniline-modified InAs. (c) Measured using 4.4 nm NCs. (d) Measured using sub 2 nm NCs.

NCs in order to observe a clear signal. We attribute this broad spectrum to the enhanced probability for aggregate formation. Figure 2 also demonstrates the known superiority of differential pulse compared to cyclic voltammetry³¹ in terms of sensitivity and signal quality hence, for the rest of the paper we present DPV rather than CV data.

In the above description of the oxidative activity of the TOP-InAs, we did not discuss the fact that the electrochemical response of NCs dispersed in salt solution is the sum of all electroactive species in the solution and the interactions between them. We were able to do so because the TOP ligand was found to be inactive in the electrochemical potential window used in the DPV measurements. This

is however not necessarily true for the conjugated and functional ligands used to surface-modify the InAs NCs.

To distinguish between the possible contribution of the ligand itself from that of the nanocrystal, we have conducted voltammetry measurements of their free ligands as well. Figure 3a,b shows the DPV of aniline-modified NCs and MTP-modified NCs in comparison to their corresponding free ligands. The NTP-modified NCs and the MoTP-modified NCs were measured in a similar manner. For Figure 3b, we do not observe any response from the MTP ligand itself and hence the interpretation is straight forward as in the TOP-InAs case. Figure 3a however shows that there is response associated with the free aniline ligand (dashed line), which

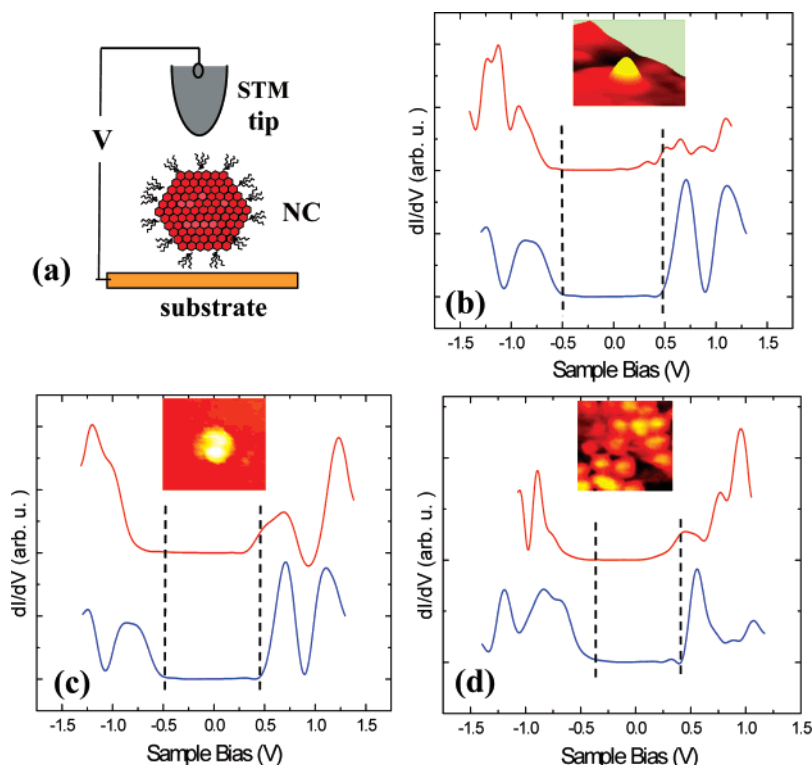


Figure 4. (a) Schematic of the STS measurement configuration. (b–d) Tunneling (dI/dV vs V) spectra of (b) a single aniline-capped InAs QD (top curve) in comparison with a single TOP-capped InAs QD (bottom curve), (c) a single MTP-modified InAs QD (top) in comparison with a single TOP-capped InAs QD (bottom) and (d) an aggregate of MTP-modified InAs QDs (top) in comparison to an aggregate of TOP-capped InAs QDs (bottom). All spectra show a shift of ~ 0.2 eV toward the valence band. The insets show the topographic images of the measured (modified) 4.4 nm diameter InAs NCs. The dashed vertical lines are guides to the eye, demonstrating the shifts of the band edges of the modified NCs toward lower energies.

is centered below to 0.8 V. Examining the response of the aniline-modified InAs (full line in Figure 3a) we note the appearance of two peaks. The low-energy peak is in good agreement with the peak position of the bare ligand (dashed line). We therefore attribute only the higher energy peak at 0.8 eV to the InAs NC HOMO.

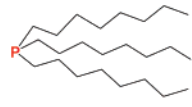
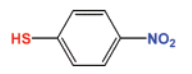
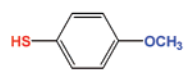
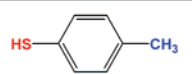
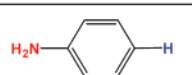
To obtain a clearer picture, we plot in Figure 3c the signal for 4.4 nm diameter TOP-capped InAs, MTP-modified InAs, and aniline-modified InAs after subtracting the background for each. This figure shows that the exchange of the TOP ligands by MTP and aniline results in a shift of the InAs NC HOMO level to lower energy (stabilization). To quantify the shifts, we fitted the relevant peaks by a Gaussian function and deduced the onset potential and the peak position. From this analysis, we find that the MTP and aniline-modified NCs are shifted by about 0.2–0.3 and 0.3–0.4 eV, respectively. Recalling that the band gap was found to remain intact upon ligand exchange, corresponding shifts are expected for the lowest unoccupied molecular orbital (LUMO). To further establish the remarkable shift observed in DPV, we also performed STS measurements of the same NCs with different surface ligands.

For scanning tunneling microscopy (STM) and STS, the NCs were deposited on an atomically flat Au(111) substrate by drop casting of InAs in toluene solution. The tunneling spectra (dI/dV versus V characteristics, proportional to the electronic density of states) were acquired by positioning and stabilizing the STM tip over a specific QD, as shown in

Figure 4a. All spectra were taken at room temperature to compare with the DPV results. This yielded significant broadening of the excited level features compared to spectra acquired at 4.2 K, presented in our previous reports (e.g., as reviewed in ref 32). However, this broadening does not affect the accuracy of the band gap assessment. We also note in passing that the spectra were taken with the STM tip retracted as far as possible from the NC to minimize the effect of voltage division between the two tunnel junction, which acts to increase the apparent (measured) gaps.³² Figure 4b–d demonstrate the effects of TOP-ligand exchange by MTP and aniline on the tunneling spectra of ~ 4.4 nm diameter InAs NCs. The upper (red) curves are typical spectra acquired on aniline-modified NC (Figure 4b) and MTP-modified NCs (isolated, Figure 4c, and within an aggregate, Figure 4d), while the lower (blue) curves were measured on TOP-capped NCs. These data show that the band gap does not change upon exchange of the capping ligands, which is in agreement with our aforementioned optical data. On the other hand, the band edges (corresponding to the HOMO and LUMO levels) for both MTP and aniline-modified NCs were found to shift toward lower energies by about 0.2 eV. This latter observation agrees qualitatively with the DPV results thus corroborating our above interpretation of the DPV findings.

After establishing the energy level tuning capabilities for NCs larger than 3 nm, we turned to examine the effect on very small (< 2 nm) NCs. For this size, of NCs we used only electrochemistry analysis, and the results are shown in

Table 1. Estimated HOMO Levels versus Vacuum (eV) and Shifting Values (eV) of InAs NCs by Means of DPV and STS^a

Modifying capping ligand	Free ligand dipole	STS meas.	DPV meas.					
			Large NCs ^a			Small NCs ^a		
			Shift	Onset	peak	width	Onset	peak
TOP 	-	0	-	-0.05	0.30	4.7 ^b	4.85 ^b	0.08
NTP 	→	-	-0.05	0.0	0.12	0.05	0.1	0.12
MoTP 	←	-	0.15	0.15	0.10	0.0	0.0	0.10
MTP 	←	0.2	0.15	0.25	0.17	0.0	0.05	0.12
aniline 	→	0.2	0.25	0.35	0.17	0.3	0.35	0.14

^a Using DPV, the energetic levels were determined through onset potential and peak potential analysis.³³ The Table includes the width, center, and onset of the Gaussian function fit. The values for the onset and center of the peak are relative to those of the TOP-coated small NC. ^bLarge NCs were ~4.4 nm diameter, small NCS were <2 nm diameter. ^cThe reference "0" levels for onset and peak potentials. The NC size was estimated using the energy of the first exciton absorption peak.

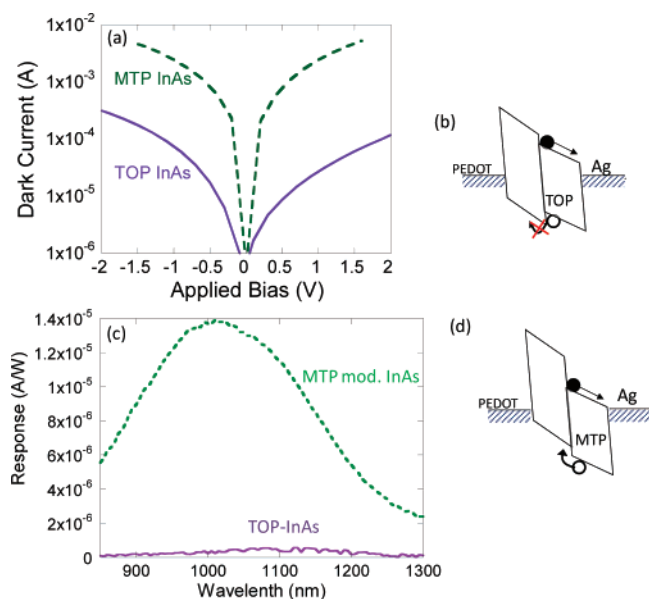


Figure 5. (a) I – V curves of single layer InAs NC devices in the dark. (b) Schematic short circuit energy level diagram of the Y-PPV|TOP–InAs device. (c) Action spectra of bilayer devices in the near IR made of yellow-PPV (Y-PPV) and InAs NCs: TOP–InAs NCs (full line), MTP-modified InAs NCs (dashed line). (d) Schematic short circuit energy level diagram of the Y-PPV| MTP-modified InAs device.

Figure 3d. The peak analysis is summarized in Table 1. The relative shift of the HOMO level between the TOP-coated large and small NCs is hard to determine due to the broad signal obtained for the TOP-coated large NCs. STS measure-

ments, reported elsewhere, showed negligible shift of the HOMO level between different sizes of TOP-coated NCs. Examining the effect of ligand exchange, we note that unlike the large NCs, for the small NCs only the aniline seems to have a significant effect on the energy level position. We defer the discussion of this to the conclusions part.

To demonstrate the technological importance of the above findings, we examined the relevance of surface ligand modifications to device functionality. The effect of using a conjugated rigid ligand, MTP, instead of the bulky and saturated TOP ligands on the interdot coupling is examined first. We have constructed single layer devices where a film of NCs was sandwiched between two electrodes. Figure 5a shows that the film composed of NCs bearing MTP ligands supports an order of magnitude higher current compared to the as-synthesized TOP–InAs-based film.

Next, to demonstrate how the remarkable surface ligand-induced shifts can be used to tune device functionality we have constructed bilayer devices composed of ITO|PEDOT|Y–PPV|NCs|Ag. We chose this composition because the HOMO level of Y-PPV is at ~5.0 eV and the HOMO level of TOP–InAs is at ~4.7 eV. Figure 5b,d schematically describes the short circuit energy band diagram of the bilayer PVs where the top layer is TOP–InAs and MTP-modified InAs, respectively, manifesting the band gap shift discussed above. We note that the energy barrier for photogenerated holes moving from the NC layer into the PPV layer is expected to be much lower for the MTP-modified InAs compared to the TOP–InAs. Figure 5c shows the action

spectra for the two devices where the response for the MTP-modified InAs is 2 orders of magnitude higher than that of the TOP-InAs. Because the transport in the MTP-modified InAs is enhanced by only ~ 1 order (see Figure 5a), the further dramatic increase (Figure 5c) by an additional order of magnitude is assigned to the effect of level shifting induced by the surface ligands.

In conclusion, we have modified the original surface layer of TOP-InAs NCs with molecules bearing different binding groups and with molecules having different auxiliary polar substituents. The exchange reaction was verified using FTIR measurements and the optical absorption gap as well as the first exciton peak showed no change following the exchange. Using differential pulse voltammetry we found that the HOMO-LUMO levels can be shifted by up to 0.3 eV. Two sample sizes (~ 4.4 nm diameter (large) and < 2 nm diameter (small)) of InAs NCs were investigated. To substantiate the DPV measurements, STS was performed on part of the samples. The importance of the energy level shift for device performance was demonstrated and showed that this method would be valuable for device engineering. Table 1 summarizes the results obtained from DPV as well as from STS.

Examining the values for the relatively large NCs along with the values for the free ligand dipole, we note that there is no consistent correlation between the energy levels shift and the value (and sign) of the free ligand dipole. In a recent theoretical publication by Deutsch et al.,²⁹ the effect of molecular dipoles assembled on surfaces was computationally analyzed and showed the following: (1) The polar molecules assembled on surfaces affect each other so as to minimize the mutual interaction. (2) There could be partial charge exchange between the anchor group and the substrate. (3) The electrostatic field of the dipole molecule affects the charge distribution below the surface. From these, it is clear that the overall effect is not necessarily directly related to the magnitude of the dipole of the unbound molecule.

The results for the large NCs show that upon exchange of the TOP with any of the other ligands the electronic energy levels of the NC were stabilized (or unchanged in the case of NTP). This implies that if we assign the energy levels shift to an effective dipole, then its positive end is pointing toward the NC center. The lack of correlation with the molecules polar terminal group suggests that the binding functionality (anchor group) plays the most important role in determining the shift. To this extent, we write the electronegativity of each of the relevant atoms at the interface: phosphorus (2.19 Pauling), sulfur (2.58 Pauling), and nitrogen (3.04 Pauling). The electronegativity of sulfur and nitrogen is significantly higher compared to phosphorus suggesting that the sulfur and nitrogen should be more efficient in drawing electrons out of the InAs and producing a dipole with a polarity that agrees with the direction of the electron energy level shift (HOMO level shift: aniline > thiol-containing ligands > TOP).

The physical picture of the below 2 nm diameter NC however does not seem to follow the explanation that we found for the "large" NCs. As Table 1 shows, for all the thiol-bound molecules there is no significant effect, while

for aniline-bound molecules the effect seems to be similar to that found for the large NCs. The essence of the explanation provided for the large NCs is that one can consider the NC as having "bulk" and surface that can be treated separately. As the NC gets smaller, this assumption becomes more and more invalid as surface interactions may extend across significant portions of the NC. Full understanding of the effects in small NCs will require dedicated modeling, which will most likely employ extensive computer resources.

In summary, the surface capping of NCs is an integral part of its electronic system and it can alter, among other things, the energy levels position. We envisage that engineering of the nanocrystals surface capping would allow tuning of energy levels alignment of a chosen nanocrystals-polymer system to arrive at better photocells and/or LEDs.

Acknowledgment. We are grateful to Professor Chaim Yarnitzky for sharing with us his knowledge and experience in electrochemistry. The authors also thank Emma Gerts for assisting in acquiring FTIR measurements and L. Kronik for fruitful discussions. This work was supported by the Israeli ministry of science. N.T. acknowledges partial support the Russell Berrie Nanotechnology Institute at the Technion. M.S.H expresses her gratitude for the financial support of the Israeli ministry of science.

Supporting Information Available: Quantum dot synthesis and ligand exchange, voltammetry measurements, and device processing. This material is free of charge via the Internet at <http://pubs.acs.org>.

References

- (1) Colvin, V. L.; Schlamp, M. C.; Alivisatos, A. P. *Nature* **1994**, *370* (6488), 354–357.
- (2) Tessler, N.; Medvedev, V.; Kazes, M.; Kan, S. H.; Banin, U. *Science* **2002**, *295* (5559), 1506–1508.
- (3) Coe, S.; Woo, W. K.; Bawendi, M.; Bulovic, V. *Nature* **2002**, *420* (6917), 800–803.
- (4) Steckel, J. S.; Coe-Sullivan, S.; Bulovic, V.; Bawendi, M. G. *Adv. Mater.* **2003**, *15* (21), 1862–1866.
- (5) Koktysh, D. S.; Gaponik, N.; Reufer, M.; Crewett, J.; Scherf, U.; Eychmuller, A.; Lupton, J. M.; Rogach, A. L.; Feldmann, J. *ChemPhysChem* **2004**, *5* (9), 1435–1438.
- (6) Greenham, N. C.; Peng, X. G.; Alivisatos, A. P. *Phys. Rev. B: Condens. Matter* **1996**, *54* (24), 17628–17637.
- (7) Huynh, W. U.; Dittmer, J. J.; Alivisatos, A. P. *Science* **2002**, *295* (5564), 2425–2427.
- (8) McDonald, S. A.; Konstantatos, G.; Zhang, S. G.; Cyr, P. W.; Klem, E. J. D.; Levina, L.; Sargent, E. H. *Nat. Mater.* **2005**, *4* (2), 138–144.
- (9) Maria, A.; Cyr, P. W.; Klem, E. J. D.; Levina, L.; Sargent, E. H. *Appl. Phys. Lett.* **2005**, *87*, (21) 213112.
- (10) Konstantatos, G.; Howard, I.; Fischer, A.; Hoogland, S.; Clifford, J.; Klem, E.; Levina, L.; Sargent, E. H. *Nature* **2006**, *442* (7099), 180–183.
- (11) Ginger, D. S.; Greenham, N. C. *Phys. Rev. B* **1999**, *59* (16), 10622–10629.
- (12) Solomeshch, O.; Kigel, A.; Saschiuk, A.; Medvedev, V.; Aharoni, A.; Razin, A.; Eichen, Y.; Banin, U.; Lifshitz, E.; Tessler, N. *J. Appl. Phys.* **2005**, *98*, (7) 074310.
- (13) Haick, H.; Ghabboun, J.; Niitsoo, O.; Cohen, H.; Cahen, D.; Vilan, A.; Hwang, J. Y.; Wan, A.; Amy, F.; Kahn, A. *J. Phys. Chem. B* **2005**, *109* (19), 9622–9630.
- (14) Visoly-Fisher, I.; Sitt, A.; Wahab, M.; Cahen, D. *ChemPhysChem* **2005**, *6* (2), 277–285.
- (15) Vilan, A.; Shanzer, A.; Cahen, D. *Nature* **2000**, *404* (6774), 166–168.

- (16) Campbell, I. H.; Kress, J. D.; Martin, R. L.; Smith, D. L.; Barashkov, N. N.; Ferraris, J. P. *Appl. Phys. Lett.* **1997**, *71* (24), 3528–3530.
- (17) Ganzorig, C.; Kwak, K. J.; Yagi, K.; Fujihira, M. *Appl. Phys. Lett.* **2001**, *79* (2), 272–274.
- (18) Khodabakhsh, S.; Sanderson, B. M.; Nelson, J.; Jones, T. S. *Adv. Funct. Mater.* **2006**, *16* (1), 95–100.
- (19) Akamatsu, K.; Tsuruoka, T.; Nawafune, H. *J. Am. Chem. Soc.* **2005**, *127* (6), 1634–1635.
- (20) Steiner, D.; Aharoni, A.; Banin, U.; Millo, O. *Nano Lett.* **2006**, *6* (10), 2201–2205.
- (21) Talapin, D. V.; Rogach, A. L.; Kornowski, A.; Haase, M.; Weller, H. *Nano Lett.* **2001**, *1* (4), 207–211.
- (22) Skaff, H.; Sill, K.; Emrick, T. *J. Am. Chem. Soc.* **2004**, *126* (36), 11322–11325.
- (23) Kucur, E.; Riegler, J.; Urban, G.; Nann, T. *J. Chem. Phys.* **2004**, *121* (2), 1074–1079.
- (24) Kucur, E.; Bucking, W.; Arenz, S.; Giernoth, R.; Nann, T. *ChemPhysChem* **2006**, *7* (1), 77–81.
- (25) Querner, C.; Reiss, P.; Sadki, S.; Zagorska, M.; Pron, A. *Phys. Chem. Chem. Phys.* **2005**, *7* (17), 3204–3209.
- (26) Aldakov, D.; Chandezon, F.; De Bettignies, R.; Firon, M.; Reiss, P.; Pron, A. *Eur. Phys. J.: Applied Physics* **2006**, *36* (3), 261–265.
- (27) Guyot-Sionnest, P.; Wang, C. *J. Phys. Chem. B* **2003**, *107* (30), 7355–7359.
- (28) Millo, O.; Katz, D.; Levi, Y.; Cao, Y. W.; Banin, U. *J. Low Temp. Phys.* **2000**, *118* (5–6), 365–373.
- (29) Deutsch, D.; Natan, A.; Shapira, Y.; Kronik, L. *J. Am. Chem. Soc.* **2007**, *129* (10), 2989–2997.
- (30) Myung, N.; Ding, Z. F.; Bard, A. J. *Nano Lett.* **2002**, *2* (11), 1315–1319.
- (31) Kissinger, P. T.; Heineman, W. R. *Laboratory techniques in electroanalytical chemistry*; Marcel Dekker: New York, 1996.
- (32) Banin, U.; Millo, O. *Annu. Rev. Phys. Chem.* **2003**, *54*, 465–492.
- (33) Kucur, E.; Riegler, J.; Urban, G. A.; Nann, T. *J. Chem. Phys.* **2003**, *119* (4), 2333–2337.

NL0732171